

# ABTS as an Electron Shuttle to Enhance the Oxidation Kinetics of Substituted Phenols by Aqueous Permanganate

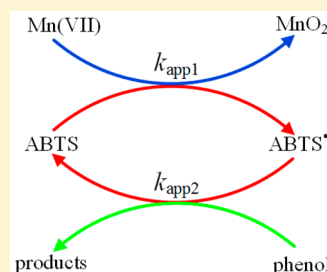
Yang Song,<sup>†</sup> Jin Jiang,<sup>\*,†</sup> Jun Ma,<sup>\*,†</sup> Su-Yan Pang,<sup>‡</sup> Yong-ze Liu,<sup>†</sup> Yi Yang,<sup>†</sup> Cong-wei Luo,<sup>†</sup> Jian-qiao Zhang,<sup>†</sup> Jia Gu,<sup>†</sup> and Wen Qin<sup>†</sup>

<sup>†</sup>State Key Laboratory of Urban Water Resource and Environment, School of Municipal and Environmental Engineering, Harbin Institute of Technology, Harbin 150090, China

<sup>‡</sup>Key Laboratory of Green Chemical Engineering and Technology of College of Heilongjiang Province, College of Chemical and Environmental Engineering, Harbin University of Science and Technology, Harbin 150040, China

## Supporting Information

**ABSTRACT:** In this study, it was, interestingly, found that 2,2'-azino-bis(3-ethylbenzothiazoline)-6-sulfonate (ABTS), a widely used electron shuttle, could greatly accelerate the oxidation of substituted phenols by potassium permanganate (Mn(VII)) in aqueous solutions at pH 5–9. This was attributed to the fact that these substituted phenols could be readily oxidized by the stable radical cation (ABTS<sup>•+</sup>), which was quickly produced from the oxidation of ABTS by Mn(VII). The reaction of Mn(VII) with ABTS exhibited second-order kinetics, with stoichiometries of ~5:1 at pH 5–6 and ~3:1 at pH 7–9, and the rate constants varied negligibly from pH 5 to 9 ( $k = (9.44 \pm 0.21) \times 10^4 \text{ M}^{-1} \text{ s}^{-1}$ ). Comparatively, the reaction of ABTS<sup>•+</sup> with phenol showed biphasic kinetics. The second-order rate constants for the reactions of ABTS<sup>•+</sup> with substituted phenols obtained in the initial phase were strongly affected by pH, and they were several orders of magnitude higher than those for the reactions of Mn(VII) with substituted phenols at each pH. Good Hammett-type correlations were found for the reactions of ABTS<sup>•+</sup> with undissociated ( $\log(k) = 2.82-4.31\sigma$ ) and dissociated phenols ( $\log(k) = 7.29-5.90\sigma$ ). The stoichiometries of  $(2.2 \pm 0.06):1$  (ABTS<sup>•+</sup> in excess) and  $(1.38 \pm 0.18):1$  (phenol in excess) were achieved in the reaction of ABTS<sup>•+</sup> with phenol, but they exhibited no pH dependency.



## INTRODUCTION

Over the past decades, permanganate (Mn(VII)) has received much more attention as a chemical oxidant to control odor and taste, algal toxins, and the formation of disinfection byproducts during water treatment due to the properties of ease of handling, stability, and low cost, as well as its wide reactivity with electron-rich organic moieties such as phenols and olefins.<sup>1–10</sup> In addition, Mn(VII) has also been applied in in-situ chemical oxidation (ISCO) to remediate contaminated groundwater and soil.<sup>11</sup>

Recently, it was found that manganese dioxide (MnO<sub>2</sub>) formed in situ upon the decomposition of Mn(VII) could accelerate the reactions of Mn(VII) with phenols.<sup>4,5</sup> A surface catalytic mechanism was proposed to account for the observed promoting effect of MnO<sub>2</sub>, where the formation of surface precursor complexes between organic pollutants and surface active sites of MnO<sub>2</sub> was involved.<sup>4,5</sup> In addition, Zhang et al. reported that ceria-supported ruthenium (Ru(III)/CeO<sub>2</sub>), a heterogeneous catalyst, could enhance the oxidation of butylparaben by Mn(VII).<sup>12</sup> This was explained by the fact that Ru(III) was oxidized by Mn(VII) to produce reactive Ru(VI) and Ru(VII) intermediates, which could participate in butylparaben degradation. However, MnO<sub>2</sub> can act as a catalyst to enhance Mn(VII) oxidation only at an acidic pH, and Ru is a precious metal in spite of its effectiveness over a wide pH range.

In this study, we will present a novel and efficient oxidation process involving Mn(VII) with metal-free ABTS (2,2'-azino-bis(3-ethylbenzothiazoline)-6-sulfonate) as a catalyst over a wide pH range. In fact, ABTS as a simple synthetic electron shuttle has been widely used as a redox mediator in enzymatic catalysis (e.g., laccase).<sup>13–16</sup> A stable green radical, ABTS<sup>•+</sup>, once formed from laccase oxidation of ABTS, has much higher reactivity than laccase itself. For instance, several groups reported that ABTS could promote laccase oxidation of polycyclic aromatic hydrocarbons (e.g., anthracene, pyrene, phenanthrene, and benzo[a]-pyrene),<sup>17–19</sup> pentachlorophenol,<sup>20</sup> and hydroxy polychlorinated biphenyls.<sup>21</sup> Camarero et al. and Murugesan et al. demonstrated that this approach was also effective in paper-pulp-bleaching wastewater treatment.<sup>22–24</sup> Hence, it seems likely that ABTS can also serve as a catalyst in the oxidation of micropollutants by Mn(VII), where ABTS and ABTS<sup>•+</sup> form a catalytic cycle.

This study was conducted to examine whether ABTS could act as a catalyst to promote the oxidation of substituted phenols by Mn(VII). To this end, the kinetics and stoichiometries of the reactions of Mn(VII) with ABTS, and ABTS<sup>•+</sup> with substituted

Received: July 13, 2015

Revised: September 11, 2015

Accepted: September 17, 2015

Published: September 17, 2015

phenols were investigated at pH 5–9 (i.e., pH = 5, 6, 7, 8, and 9) first. Furthermore, the Hammett-type correlations were developed for the reactions of ABTS<sup>•+</sup> with undissociated and dissociated phenols and compared with those of other water-treatment oxidants. Finally, the effects of trace levels of ABTS on the oxidation of substituted phenols by Mn(VII) as well as other oxidants (i.e., ferrate (Fe(VI)) and hypochlorous acid (HOCl)) were examined in synthetic and natural waters. In addition, detailed kinetic and mechanistic aspects for the reaction of Mn(VII) with ABTS, a model system for the initial one-electron transfer process, obtained in this study were expected to provide useful information for a better understanding of the fates of manganese intermediates involved in Mn(VII) oxidation, as did in the case of Fe(VI) by Lee et al.<sup>25</sup>

## ■ EXPERIMENTAL SECTION

**Standards and Reagents.** Phenol, 4-chlorophenol, 4-bromophenol, 4-carboxyphenol, 4-methylphenol, and 4-fluorophenol were all obtained from Sigma-Aldrich with a purity of 99%. Suwannee River Humic Acid (SRHA) was obtained from International Humic Substances Society. Other chemicals of analytical grade or higher were purchased from Sigma-Aldrich and Sinopharm Chemical Reagent Co., Ltd. Deionized water (18.2 MΩ·cm) was obtained by the passage of distilled water through a Millipore Milli-Q water purification system. A natural water sample was taken from Songhua River in Harbin, China (DOC = 6.4 mg C/L, alkalinity = 190 mg/L as CaCO<sub>3</sub>, and pH = 7.8). After filtering through the glass fiber filters of 0.7 μm nominal pore size (Whatman GF/F), this water was buffered to pH 8 with borate buffer (10 mM) and stored at 4 °C.<sup>8</sup>

Weighed amounts of potassium permanganate crystals were dissolved to make Mn(VII) stock solutions, which were standardized spectrophotometrically by the direct 525 nm method ( $\epsilon = 2500 \text{ (M}^{-1} \text{ cm}^{-1})$ ). Potassium ferrate (K<sub>2</sub>FeO<sub>4</sub>) with high purity was prepared by the method of Thompson et al.<sup>26</sup> Solid samples of K<sub>2</sub>FeO<sub>4</sub> were dissolved in borate buffered solutions (pH ≈ 9.1) to make stock solutions of Fe(VI), which were determined by the direct 510 nm method ( $\epsilon = 1150 \text{ (M}^{-1} \text{ cm}^{-1})$ ) after filtration to remove ferric particulates.<sup>27,28</sup> Stock solutions of HOCl were prepared by diluting a commercial solution (5.2% active chlorine) and were determined by iodometry.<sup>29</sup> ABTS stock solutions were freshly prepared by dissolving ABTS solids into deionized water.<sup>25,30,31</sup> ABTS<sup>•+</sup> stock solutions were freshly prepared following the suggestion of Re et al.<sup>32</sup> by the stoichiometric reaction between ABTS and potassium persulfate (K<sub>2</sub>S<sub>2</sub>O<sub>8</sub>) and were standardized spectrophotometrically at 415 nm ( $\epsilon = 34000 \text{ (M}^{-1} \text{ cm}^{-1})$ ).<sup>30,31</sup>

**Reaction Kinetics and Stoichiometries.** All of the experiments were performed over the pH range of 5–9 (i.e., pH = 5, 6, 7, 8, and 9) at 25 ± 1 °C. The following buffers (10 mM) were used: sodium acetate for pH 5–6 (i.e., pH = 5 and 6), and sodium borate for pH 7–9 (i.e., pH = 7, 8, and 9). Although the buffering capacities were weak for pH 6 and 7, pH values changed negligibly during the reactions. MOPS and phosphate with much stronger buffering capacities for pH 6 and 7 were not used due to their interferences with Mn(VII) reactions.<sup>4</sup>

The reaction kinetics of Mn(VII) with ABTS were investigated by monitoring the formation of ABTS<sup>•+</sup> at 415 nm with a stopped-flow spectrophotometer, where the pseudo-first-order reaction conditions with ABTS in excess were maintained. To eliminate the interference of the accumulation of MnO<sub>2</sub> formed in situ at pH 7–9, we added excess sodium pyrophosphate into the reaction solutions, where soluble Mn(III) rather than MnO<sub>2</sub>

was formed.<sup>33</sup> The molar absorption coefficient of Mn(III)–pyrophosphate complex at 415 nm was so low ( $\sim 50 \text{ (M}^{-1} \text{ cm}^{-1})$ ) for Mn(III)–pyrophosphate versus 34 000  $\text{(M}^{-1} \text{ cm}^{-1})$  for ABTS<sup>•+</sup>) that its contribution to the absorbance at 415 nm was negligible.<sup>31</sup> Similarly, the reaction kinetics of ABTS<sup>•+</sup> with substituted phenols were examined at pH 5–9 (i.e., pH = 5, 6, 7, 8, and 9) by monitoring the decay of ABTS<sup>•+</sup> at 415 nm with stopped-flow spectrophotometer, where the pseudo-first-order reaction conditions with substituted phenols in excess were maintained.

The stoichiometries for the reaction of Mn(VII) with ABTS at pH 5–9 (i.e., pH = 5, 6, 7, 8, and 9) were determined in the absence and presence of pyrophosphate by monitoring the production of ABTS<sup>•+</sup> at 415 nm with a UV–vis spectrometer. Sufficient time was allowed for the reactions to reach completion (i.e., Mn(VII) was consumed completely). In the absence of pyrophosphate, ABTS<sup>•+</sup> was detected after filtering through 0.45 μm glass fiber filters to eliminate the interference of MnO<sub>2</sub>. Similar procedures were used to examine the stoichiometries for the reaction of ABTS<sup>•+</sup> with phenol.

Further experiments were conducted to examine the effects of ABTS in trace levels on the oxidation kinetics of selected substituted phenols in synthetic or natural water by Mn(VII). Reactions were initiated by quickly spiking Mn(VII) into pH-buffered solutions containing one selected phenolic compound and ABTS at desired concentrations, where the pseudo-first-order reaction conditions were maintained with Mn(VII) in excess. Samples were collected periodically and quenched with ascorbic acid before high-performance liquid chromatography (HPLC) analysis. Comparatively, the effects of ABTS on the oxidation of phenol by Fe(VI) or HOCl in synthetic water were also examined following the same procedure as that in the case of Mn(VII).

All experiments were conducted in duplicates or triplicates, and the average data and their standard deviations were shown.

**Analytical Methods.** Phenols were determined using a HPLC equipped with a Waters symmetry C18 column, a Waters 717 autosampler, and a Waters 2487 dual λ detector. The measurement of UV–vis spectra was performed on a Cary 300 spectrometer. A stopped-flow spectrophotometer (SX20, Applied Photophysics Ltd.) equipped with both photodiode array (PDA) and photomultiplier tube (PMT) detectors was used to carry out the kinetic studies.

## ■ RESULTS AND DISCUSSION

**ABTS<sup>•+</sup> Formation in the Reaction of Mn(VII) with ABTS. Stoichiometries.** The apparent stoichiometric relationships in the reaction of Mn(VII) with ABTS were determined by the ratio ( $r_1$ ) of ABTS<sup>•+</sup> produced ( $\Delta\text{ABTS}^{\bullet+}$ ) to Mn(VII) consumed ( $\Delta\text{Mn(VII)}$ ) over the wide pH range of 5–9 in the absence and presence of pyrophosphate, respectively.

(1). *Without Pyrophosphate.* In the absence of pyrophosphate, 5 μM Mn(VII) reacted with ABTS in excess (i.e., [ABTS] = 100–300 μM) yielding 25 μM and 15 μM ABTS<sup>•+</sup> at pH 5–6 and pH 7–9, respectively. These data suggested that Mn(II) (i.e., aqua-Mn<sup>2+</sup>) was the final manganese product at pH 5–6, while the colloidal MnO<sub>2</sub> product was formed at pH 7–9. The higher stoichiometries at pH 5–6 were mainly due to the fact that colloidal MnO<sub>2</sub> could readily oxidize ABTS, which was confirmed in the experiments (data were not shown).

The possible pathways for the generation of ABTS<sup>•+</sup> from the reaction between Mn(VII) and ABTS are proposed. First, the

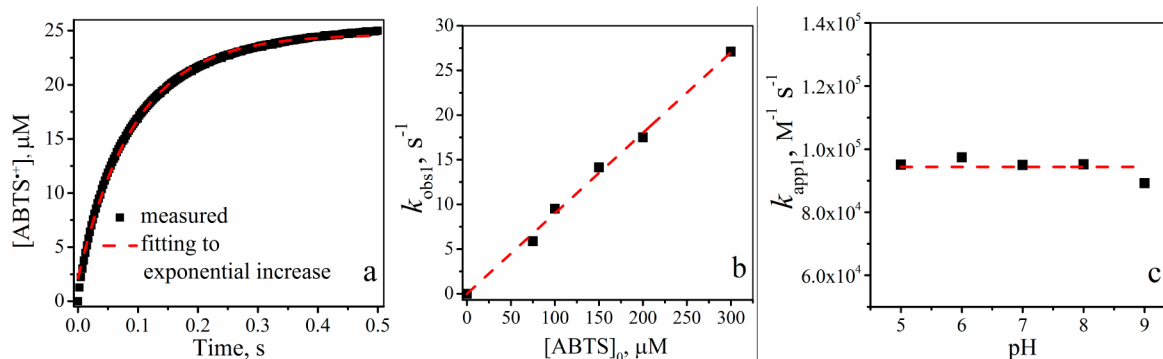
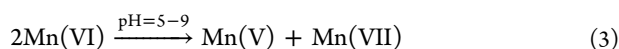
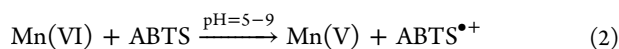


**Figure 1.** Formation of  $\text{ABTS}^{\bullet+}$  (415 nm) from the reaction of  $\text{Mn(VII)}$  ( $5 \mu\text{M}$ ) with  $\text{ABTS}$  ( $100 \mu\text{M}$ ) at pH 5 (a), a linear plot of the pseudo-first-order rate constants ( $k_{\text{obs}}$ ) for the formation of  $\text{ABTS}^{\bullet+}$  vs  $\text{ABTS}$  concentration at pH 5 (b), and the second-order rate constants ( $k_{\text{app}}$ ) for the reaction of  $\text{Mn(VII)}$  with  $\text{ABTS}$  over the pH range of 5–9 (c). The black symbols represent the experimental data, and the red dashed lines represent the model prediction.

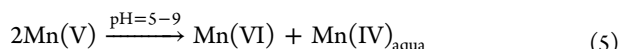
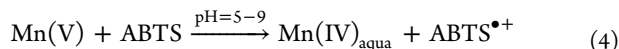
oxidation of  $\text{ABTS}$  by  $\text{Mn(VII)}$  via a one-electron transfer process produces  $\text{ABTS}^{\bullet+}$  and  $\text{Mn(VI)}$  (eq 1).



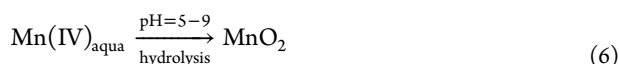
Then,  $\text{Mn(VI)}$  may react with  $\text{ABTS}$ , forming  $\text{Mn(V)}$  (eq 2) or self-decay into  $\text{Mn(V)}$  and  $\text{Mn(VII)}$  (eq 3).<sup>34–36</sup>



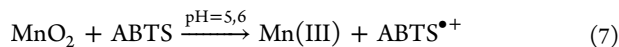
$\text{Mn(V)}$  may also participate in the oxidation of  $\text{ABTS}$ , producing  $\text{Mn(IV)}_{\text{aqua}}$  (i.e.,  $\text{aqua-MnO}^{2+}$ ) (eq 4) or self-decompose into  $\text{Mn(VI)}$  and  $\text{Mn(IV)}_{\text{aqua}}$  (eq 5).<sup>37–39</sup>



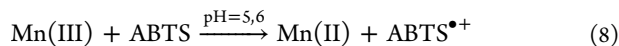
Then,  $\text{Mn(IV)}_{\text{aqua}}$  hydrolyzes into colloidal  $\text{MnO}_2$  quickly without a complexing ligand (eq 6).<sup>39,40</sup>



At acidic pH, colloidal  $\text{MnO}_2$  can readily oxidize  $\text{ABTS}$  producing  $\text{Mn(III)}$  (i.e.,  $\text{aqua-Mn}^{3+}$ ) (eq 7).<sup>40</sup>



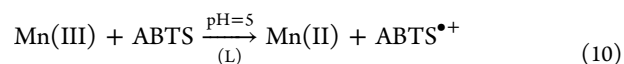
Then, the intermediate product,  $\text{Mn(III)}$ , reacts with  $\text{ABTS}$ , forming  $\text{Mn(II)}$  (eq 8) or disproportionates into  $\text{Mn(II)}$  and  $\text{Mn(IV)}_{\text{aqua}}$  (eq 9).<sup>33</sup>



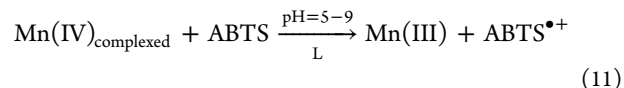
Thus, it is not difficult to understand that  $\text{Mn(II)}$  was generated as the final manganese product at acidic pH, while  $\text{MnO}_2$  colloids were formed at neutral and alkaline pH.

(2). *With Pyrophosphate (L).* In the presence of pyrophosphate (i.e., 100 and 200  $\mu\text{M}$ ), the  $r_1$  values were 5:1 and 4:1 at pH 5 and pH 6–9, respectively. These results indicated that  $\text{Mn(II)}$  (i.e., pyrophosphate-complexed  $\text{Mn}^{2+}$ ) was the final manganese product at acidic pH 5, while the soluble  $\text{Mn(III)}$  (i.e., pyrophosphate-complexed  $\text{Mn}^{3+}$ ) product was formed at pH

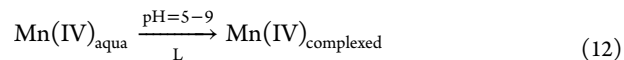
6–9.<sup>33</sup> The higher stoichiometry at pH 5 was mainly ascribed to the fact that soluble  $\text{Mn(III)}$  could readily oxidize  $\text{ABTS}$  (eq 10), which was also confirmed in the experiments (data were not shown).



Soluble  $\text{Mn(III)}$  may be formed via a one-electron transfer process from  $\text{Mn(IV)}_{\text{complexed}}$  (i.e., pyrophosphate-complexed  $\text{MnO}^{2+}$ ) (eq 11).



It is reasonable that  $\text{Mn(IV)}_{\text{complexed}}$  is generated in the presence of pyrophosphate (eq 12), which may retard the hydrolysis of  $\text{Mn(IV)}_{\text{aqua}}$  into colloidal  $\text{MnO}_2$ .



The possible occurrence of  $\text{Mn(IV)}_{\text{complexed}}$  was consistent with the studies of von Gunten and Reisz et al.<sup>38,39</sup> These authors found that in the reaction of  $\text{Mn(II)}$  with ozone in distilled water, colloidal  $\text{MnO}_2$  was observed without a complexing ligand, while  $\text{Mn(VII)}$  was generated with complexing ligands (e.g., polyphosphate and oxalate) via a complexed  $\text{MnO}^{2+}$  intermediate.<sup>38,39</sup> Hence, it can be rationalized by assuming that the oxidation of  $\text{ABTS}$  by  $\text{Mn(IV)}_{\text{complexed}}$  is faster than its hydrolysis into nonreactive colloidal  $\text{MnO}_2$ . Pathways for the formation of  $\text{Mn(IV)}_{\text{aqua}}$  in the reaction between  $\text{Mn(VII)}$  and  $\text{ABTS}$  in the presence of pyrophosphate are similar to those in the absence of pyrophosphate (eqs 1–5).

Comparatively, Lee et al. found that the stoichiometric factor (i.e., 1) of the reaction between  $\text{Fe(VI)}$  and  $\text{ABTS}$  was less than the theoretical one (i.e., 3).<sup>25,31</sup> This result was explained by the fact that  $\text{Fe(V)}$  formed upon one-electron reduction of  $\text{Fe(VI)}$  by  $\text{ABTS}$  self-decayed quickly (to  $\text{Fe(III)}$  and  $\text{H}_2\text{O}_2$ ) rather than was involved in the formation of  $\text{ABTS}^{\bullet+}$ .<sup>25</sup> This finding was markedly different from the reaction between  $\text{Mn(VII)}$  and  $\text{ABTS}$ , where manganese intermediates, as the sequential one-electron equivalent reducing products of  $\text{Mn(VII)}$  by  $\text{ABTS}$ , all participated in the oxidation of  $\text{ABTS}$ .

*Kinetics.* Figure 1a typically shows the  $\text{ABTS}^{\bullet+}$  production from the reaction of 5  $\mu\text{M}$   $\text{Mn(VII)}$  with 100  $\mu\text{M}$   $\text{ABTS}$  at pH 5 as a function of time. The kinetic data followed exponential rate law (red dashed line in Figure 1a), indicating that the reaction

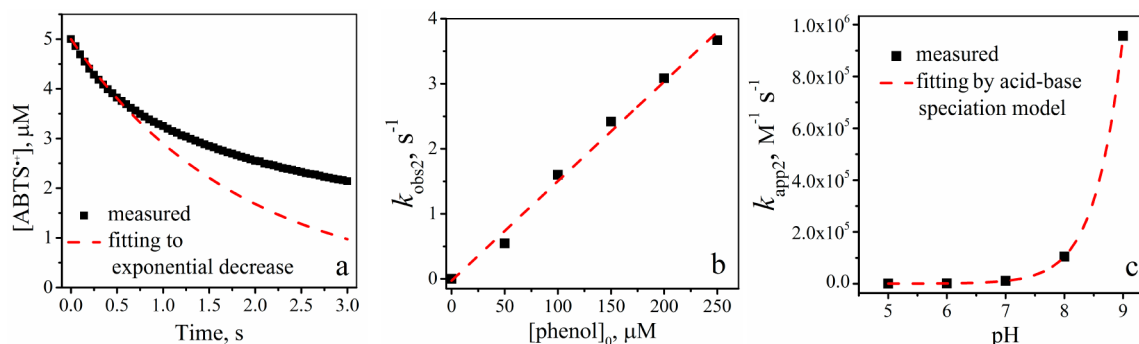


**Figure 2.** Decay of  $\text{ABTS}^{\bullet+}$  ( $5 \mu\text{M}$ ) in the presence of phenol ( $50 \mu\text{M}$ ) at pH 7 (a), a linear plot of the pseudo-first-order rate constants ( $k_{\text{obs}2}$ ) in the initial phase for the decay of  $\text{ABTS}^{\bullet+}$  vs phenol concentration at pH 7 (b), and pH-dependent second-order rate constants ( $k_{\text{app}2}$ ) for the reaction of  $\text{ABTS}^{\bullet+}$  with phenol (c). The black symbols represent the experimental data, and the red dashed lines represent the model predictions.

was first-order with respect to the  $\text{Mn}(\text{VII})$  concentration. Pseudo-first-order rate constants ( $k_{\text{obs}1}$ ,  $\text{s}^{-1}$ ) were calculated by the exponential regression (with the SX20 operating software) of  $\text{ABTS}^{\bullet+}$  production kinetic curves according to Lee's method.<sup>25</sup> The  $k_{\text{obs}1}$  values were found to vary linearly with ABTS concentrations ( $75\text{--}300 \mu\text{M}$ ) (Figure 1b), suggesting a first-order dependence on ABTS concentration. Hence, the reaction of  $\text{Mn}(\text{VII})$  with ABTS could be described by the second-order kinetics (Text S1), with the apparent second-order rate constants ( $k_{\text{app}1}$ ,  $\text{M}^{-1} \text{s}^{-1}$ ) obtained by dividing the  $k_{\text{obs}1}$  value by ABTS concentration. As shown in Figure 1c, the  $k_{\text{app}1}$  value changed negligibly at pH 5–9 ( $\sim 9.44 \times 10^4 \text{M}^{-1} \text{s}^{-1}$ ). Comparatively, Lee et al. found that the reaction of  $\text{Fe}(\text{VI})$  with ABTS was also first-order with respect to each reactant but varied significantly over the pH range of 1.5–10.<sup>25</sup>

**Reaction of  $\text{ABTS}^{\bullet+}$  with Phenol. Kinetics.** Figure 2a shows a typical time course of the oxidation kinetics of  $50 \mu\text{M}$  phenol by  $5 \mu\text{M}$   $\text{ABTS}^{\bullet+}$  at pH 7. Interestingly, the decay of  $\text{ABTS}^{\bullet+}$  exhibited biphasic kinetics (i.e., an initial phase and a secondary lag phase). Similar biphasic kinetics for the reactions of  $\text{ABTS}^{\bullet+}$  with catechin, ferulic acid, and coniferyl alcohol were also found by Tian et al.<sup>41</sup>

In the initial phase, the loss rate of  $\text{ABTS}^{\bullet+}$  followed the pseudo-first-order kinetics with excess phenol, indicating the first-order with respect to  $\text{ABTS}^{\bullet+}$ . Measured pseudo-first-order rate constants ( $k_{\text{obs}2}$ ,  $\text{s}^{-1}$ ) varied linearly with phenol concentrations ( $50\text{--}250 \mu\text{M}$ ) (Figure 2b), demonstrating a first-order with respect to phenol concentration. Hence, the reaction of  $\text{ABTS}^{\bullet+}$  with phenol displayed the second-order kinetics in the initial phase (Text S2), and the apparent second-order rate constants ( $k_{\text{app}2}$ ,  $\text{M}^{-1} \text{s}^{-1}$ ) were provided in Figure 2c. It was shown that the  $k_{\text{app}2}$  value significantly increased with the increase of solution pH from 5 to 9 ( $5.4 \times 10^2$  to  $9.57 \times 10^5 \text{M}^{-1} \text{s}^{-1}$ ). This pH dependency of  $k_{\text{app}2}$  could be explained by parallel reactions of  $\text{ABTS}^{\bullet+}$  ( $\text{ABTS}^{\bullet+}$ ;  $\text{p}K_{\text{a}} < 0$ ) with acid–base species of phenol ( $\text{p}K_{\text{a}} = 9.99$ ).<sup>42,43</sup> Accordingly, the  $k_{\text{app}2}$  value is given by

$$k_{\text{app}2} = \sum_{j=1,2}^{i=1} k_{ij} \alpha_i \beta_j \quad (13)$$

where  $\alpha_i$  and  $\beta_j$  represent the fractions of  $\text{ABTS}^{\bullet+}$  and phenol present as the species  $i$  and  $j$  at a given pH, respectively, and the  $k_{ij}$  value represents the species-specific second-order rate constant for each  $i$  and  $j$  pair. The  $k_{ij}$  values ( $k_{11}$  and  $k_{12}$ ) were determined by a nonlinear least-squares regression (acid–base speciation model) of the experimental  $k_{\text{app}2}$  values (Figure 2c). The result

showed that the  $k_{11}$  value ( $4.74 \times 10^2 \text{M}^{-1} \text{s}^{-1}$ ) was much lower than the  $k_{12}$  value ( $1.03 \times 10^7 \text{M}^{-1} \text{s}^{-1}$ ), which was consistent with the fact that the protonated phenol ( $\text{PhOH}$ ) was considerably less reactive than the phenolate anion ( $\text{PhO}^-$ ).<sup>44–47</sup>

In the secondary phase, the loss rate of  $\text{ABTS}^{\bullet+}$  slowed as the reaction progressed and deviated from the pseudo-first-order kinetics, which might be attributed to the gradual accumulation of unreacted ABTS ( $\text{ABTS}_u$ ). The inner-electron-exchange process between  $\text{ABTS}^{\bullet+}$  and  $\text{ABTS}_u$ , with an electron-exchange rate constant of  $(4 \pm 1) \times 10^7 \text{M}^{-1} \text{s}^{-1}$  in neutral aqueous solution, was found by Scott et al.<sup>42</sup> Hence, it was likely that  $\text{ABTS}_u$  had the inhibiting effect on the reaction of  $\text{ABTS}^{\bullet+}$  with phenol. To verify this, we conducted experiments to examine the effect of  $\text{ABTS}_u$  on the oxidation of phenol by  $\text{ABTS}^{\bullet+}$  with different ratios of additional  $\text{ABTS}_u$  to initial  $\text{ABTS}^{\bullet+}$  (i.e.,  $m = 0/1, 1/1, 2/1, 3/1, 4/1, 5/1$ , and  $9/1$ ) (discussed in Text S2 in detail). The results (Figure 3) showed that the consumption rate

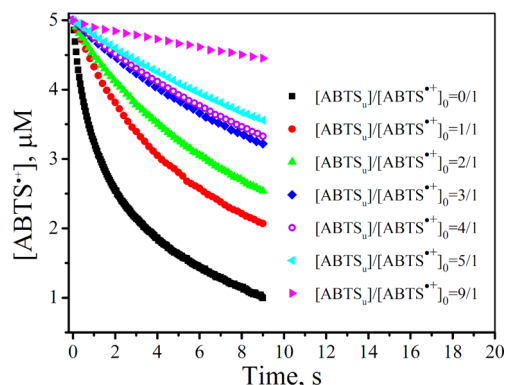


**Figure 3.** Decay of  $\text{ABTS}^{\bullet+}$  ( $5 \mu\text{M}$ ) with different ratios of  $[\text{ABTS}_u]$  to  $[\text{ABTS}^{\bullet+}]_0$  in the presence of phenol ( $50 \mu\text{M}$ ) at pH 7.

of  $\text{ABTS}^{\bullet+}$  by phenol significantly decreased with the increase in  $m$  value. Similar suppressive effects of  $\text{ABTS}_u$  over the wide pH values were shown in Figure S1.

**Stoichiometries.** The stoichiometric relationships in the reaction of  $\text{ABTS}^{\bullet+}$  with phenol were determined by the ratio ( $r_2$ ) of  $\text{ABTS}^{\bullet+}$  consumed ( $\Delta\text{ABTS}^{\bullet+}$ ) to phenol lost ( $\Delta\text{phenol}$ ) over the wide pH range of 5–9. The  $r_2$  value was found to be  $2.2 \pm 0.06$  and  $1.38 \pm 0.18$  in the cases of less and excess phenol, respectively, which changed negligibly with different pH values (Table S3). The finding that the  $r_2$  value was higher than the theoretical value of 1 in both cases suggested that oxidation products of phenol could competitively consume the oxidant

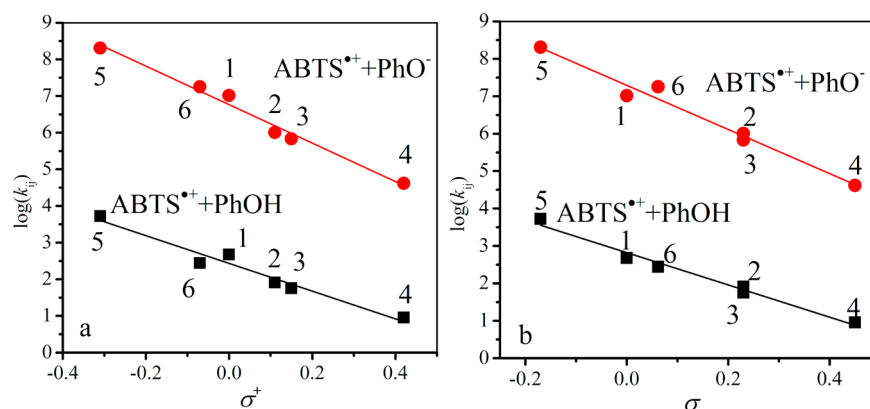


**Figure 4.** Correlations between the second-order rate constants for the reactions of  $\text{ABTS}^{\bullet+}$  ( $[\text{ABTS}_a] = 0 \mu\text{M}$ ) with undissociated phenols ( $k_{11}$ ) and dissociated phenols ( $k_{12}$ ) vs Hammett  $\sigma^+$  (a) and  $\sigma$  constants (b). The numbers of the compounds from 1 to 6 correspond to phenol, 4-chlorophenol, 4-bromophenol, 4-carboxyphenol, 4-methylphenol, and 4-fluorophenol, respectively.

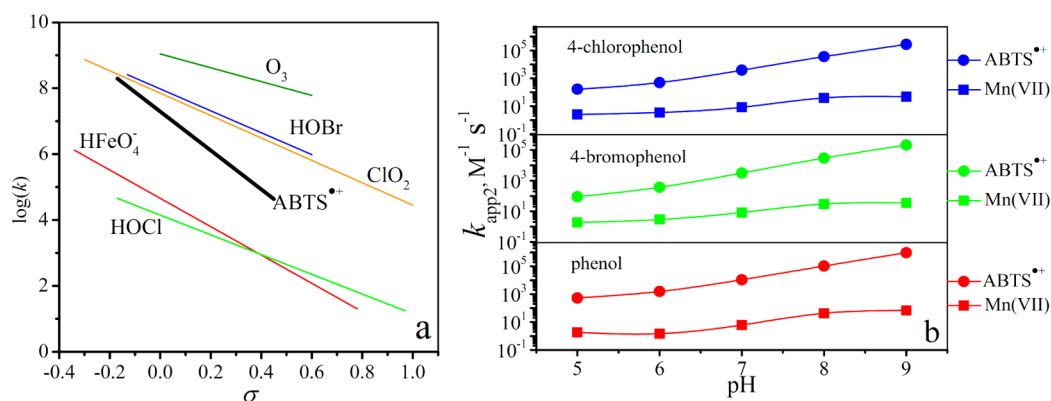


**Figure 5.** Comparison of the Hammett-type correlations for the reactions of oxidants with dissociated phenols (a) and comparison of the  $k_{\text{app}2}$  values for the reactions of  $\text{ABTS}^{\bullet+}$  ( $[\text{ABTS}_a] = 0 \mu\text{M}$ ) vs  $\text{Mn(VII)}$  with phenol, 4-chlorophenol, and 4-bromophenol at pH 5–9 (b). The correlations for  $\text{O}_3$ ,  $\text{HOBr}$ ,  $\text{ClO}_2$ ,  $\text{HFeO}_4^-$ , and  $\text{HOCl}$  in panel (a) were taken from ref 49, and the  $k_{\text{app}2}$  values for the reactions of  $\text{Mn(VII)}$  with phenol, 4-chlorophenol, and 4-bromophenol were taken from refs 4, 52, and 8, respectively.

$\text{ABTS}^{\bullet+}$ . Further, the result that the  $r_2$  value in the case of less phenol (i.e.,  $2.2 \pm 0.06$ ) was higher than that in the case of excess phenol (i.e.,  $1.38 \pm 0.18$ ) might be attributed to the stronger competition of oxidation products of phenol for  $\text{ABTS}^{\bullet+}$  in the case of less phenol vs excess phenol.

**Kinetics for the Reactions of Substituted Phenols with  $\text{ABTS}^{\bullet+}$  and Linear Free Energy Relationships.** The apparent second-order rate constants ( $k_{\text{app}2}$ ,  $\text{M}^{-1} \text{s}^{-1}$ ) for the reactions of  $\text{ABTS}^{\bullet+}$  with different phenolic compounds (phenol, 4-chlorophenol, 4-bromophenol, 4-carboxyphenol, 4-methylphenol, and 4-fluorophenol) were determined by stopped-flow spectrophotometer at pH 5–9. The  $k_{\text{app}2}$  data were shown in Figure S4. Similar to the case of phenol, the observed pH dependency of  $k_{\text{app}2}$  for these substituted phenols can be described by eq 13. The calculated specific second-order rate constants,  $k_{11}$  and  $k_{12}$ , were summarized in Table S4. The Hammett substituent constants ( $\sigma^+$ ,  $\sigma$ , and  $\sigma^-$ ) were used to predict the effect of the substituents on the rate constants of the substituted phenols.<sup>48</sup> The Hammett-type correlations were analyzed for the obtained  $k_{11}$  and  $k_{12}$  data. The better Hammett-type correlations were obtained by using  $\sigma^+$  or  $\sigma$  and shown in Figure 4 (see Text S3 for more details). The linear regressions for both undissociated and dissociated substituted phenols are shown as

$$\log(k_{11}) = 2.43 (\pm 0.08) - 3.78 (\pm 0.38) \cdot \sigma^+ \quad R^2 = 0.961 \quad (14)$$

$$\log(k_{12}) = 6.77 (\pm 0.08) - 5.25 (\pm 0.34) \cdot \sigma^+ \quad R^2 = 0.983 \quad (15)$$

$$\log(k_{11}) = 2.82 (\pm 0.07) - 4.31 (\pm 0.29) \cdot \sigma \quad R^2 = 0.982 \quad (16)$$

$$\log(k_{12}) = 7.29 (\pm 0.11) - 5.90 (\pm 0.46) \cdot \sigma \quad R^2 = 0.976 \quad (17)$$

The negative  $\rho$  value reflects the sensitivity of the reaction to the substituent effect.<sup>48</sup> Reactions of  $\text{ABTS}^{\bullet+}$  with dissociated substituted phenols (e.g.,  $\rho = -5.90$  in the case of  $\sigma$ ) were more sensitive to the substituent effect than those with undissociated substituted phenols (e.g.,  $\rho = -4.31$  in the case of  $\sigma$ ).

The Hammett-type correlations of  $\text{ABTS}^{\bullet+}$  were compared with those of other water treatment oxidants, such as  $\text{Fe(VI)}$ , ozone ( $\text{O}_3$ ), chlorine dioxide ( $\text{ClO}_2$ ), hypobromous acid ( $\text{HOBr}$ ), and  $\text{HOCl}$ .<sup>45,49–51</sup> Because  $\sigma$  was usually used to obtain Hammett-type correlations for most water treatment oxidants, Hammett-type correlations based on  $\sigma$  rather than  $\sigma^+$  were compared. Figure 5a shows that most of the  $k_{12}$  values of  $\text{ABTS}^{\bullet+}$  are several orders of magnitude greater than those of  $\text{Fe(VI)}$  and  $\text{HOCl}$  but much lower than those of  $\text{O}_3$ ,  $\text{HOBr}$ , and  $\text{ClO}_2$ . The Hammett slope for  $\text{ABTS}^{\bullet+}$  ( $\rho = -5.9$ ) was higher

than the values obtained for  $O_3$  ( $\rho = -2.1$ ),  $HOCl$  ( $\rho = -3.0$ ),  $HOBr$  ( $\rho = -3.3$ ),  $ClO_2$  ( $\rho = -3.4$ ), and  $Fe(VI)$  ( $\rho = -4.3$ ), suggesting that  $ABTS^{\bullet+}$  was more sensitive to substitution effects than the other oxidants.

Because no linear free energy relationships for  $Mn(VII)$  were found,<sup>1</sup> the  $k_{app2}$  values at each pH (rather than the Hammett-type correlation of  $ABTS^{\bullet+}$ ) were compared with those of  $Mn(VII)$ . As shown in Figure 5b, the  $k_{app2}$  values for  $Mn(VII)$  at pH 5–9 obtained from the literatures (e.g., phenol, 4-chlorophenol, and 4-bromophenol) were much lower than those for  $ABTS^{\bullet+}$ .<sup>4,8,52</sup> Hence, it is expected that trace levels of ABTS may catalyze the reactions of  $Mn(VII)$  with phenols.

**Effect of ABTS on the Oxidation Kinetics of Substituted Phenols by  $Mn(VII)$ .** Further experiments were conducted to examine the effect of ABTS on the oxidation of phenol in synthetic water by  $Mn(VII)$ . As shown typically in Figure 6, the

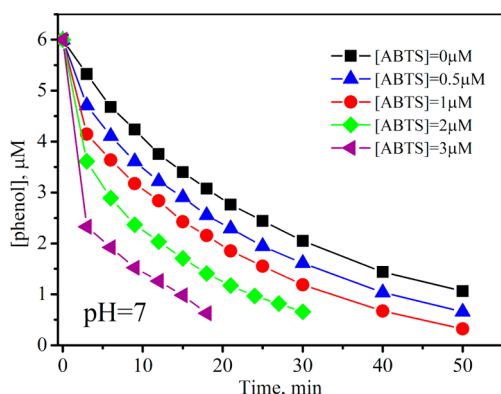


**Figure 6.** Oxidation kinetics of 6  $\mu M$  phenol by 70  $\mu M$   $Mn(VII)$  at pH 7 with different concentrations of ABTS (0–3  $\mu M$ ).

presence of trace levels of ABTS could significantly enhance the oxidation of phenol by  $Mn(VII)$  at pH 7. A similar enhancing effect of ABTS was also found on the reactions between  $Mn(VII)$  and selected substituted phenols, with an electron-donating substituent (i.e.,  $-CH_3$ ) and electron-withdrawing substituents (i.e.,  $-F$ ,  $-Cl$ ,  $-Br$ , and  $-COOH$ ) (Figure S7). A catalytic role of the  $ABTS^{\bullet+}$  and ABTS pair could describe the effect of trace levels of ABTS in promoting  $Mn(VII)$  oxidation of phenol. For the catalytic reaction to occur, the formation of  $ABTS^{\bullet+}$  by the fast reaction of  $Mn(VII)$  with ABTS is necessary. Afterward, phenol is quickly oxidized by  $ABTS^{\bullet+}$  with a much higher rate than that for the reaction of  $Mn(VII)$  with phenol, which is followed by the regeneration of ABTS.

(1). **ABTS Concentration.** The enhancing effect of ABTS at different concentrations (0.5–3  $\mu M$ ) was evaluated by comparing the half-life ( $t_{1/2}$ , min) or pseudo-first-order rate constants ( $k_{obs3}$ ,  $min^{-1}$ ). The results indicated that measured  $t_{1/2}$  values decreased and calculated  $k_{obs3}$  values increased with the increase of the ABTS concentration at each pH 5–9, respectively (Table S5). At a constant pH value, high levels of initial ABTS result in the fast formation of  $ABTS^{\bullet+}$  and, thus, the rapid oxidation of phenol by  $Mn(VII)$ .

(2). **Solution pH.** ABTS could enhance the oxidation of phenol by  $Mn(VII)$  over a wide pH range (Figure 6 for pH 7 and Figure S8 for other selected pH). Because the reactivity of  $ABTS^{\bullet+}$  with phenol increased with the increase of pH value (Figure 2c), it is expected that the promoting effect of ABTS on the oxidation of phenol by  $Mn(VII)$  is more significant at high pH than that at low pH. However, the observed enhancing effect of ABTS was not

marked in our experiments at alkaline pH (Figure S8). This discrepancy might be attributed to the fact that the higher  $k_{app2}$  value than  $k_{app1}$  at pH 8 and 9 would result in high ratios of  $ABTS_u$  to  $ABTS^{\bullet+}$ , thus reducing the oxidation rate of phenol by  $ABTS^{\bullet+}$ .

(3). **Phenol Concentration.** Further experiments for the oxidation of phenol at different initial concentrations by the  $Mn(VII)$  and ABTS combination were examined. The lower initial concentration of phenol was added, and the higher loss rate of phenol was found at a constant pH value and an ABTS concentration (Figure S9). One possible explanation was that the concentrations of phenol had influence on the ratio of  $ABTS_u$  to  $ABTS^{\bullet+}$  (i.e., low concentrations of phenol resulting in low ratios of  $ABTS_u$  to  $ABTS^{\bullet+}$ ; see Text S4 for more details).

**The Role of ABTS in the Oxidation of Substituted Phenols by Other Oxidants.** The results above suggest that ABTS can accelerate the reactions of  $Mn(VII)$  with substituted phenols due to the higher  $k_{app2}$  values of their oxidation by  $ABTS^{\bullet+}$  versus  $Mn(VII)$  (Figure 5b). Similarly, because the rates for the oxidation of substituted phenols by  $ABTS^{\bullet+}$  are much higher than those of  $Fe(VI)$  and  $HOCl$  (Figure 5a), it is expected that ABTS can also catalyze the oxidation by these mild oxidants. To identify this, we conducted experiments to examine the effect of ABTS on the oxidation kinetics of phenol by  $Fe(VI)$  and  $HOCl$ . As shown in Figure S10a, ABTS greatly accelerated the kinetics of  $Fe(VI)$  with phenol as expected. However, no obvious enhancement of ABTS on the reaction of  $HOCl$  with phenol (Figure S10b) was found. This was ascribed to the fairly low generation rate of  $ABTS^{\bullet+}$  from the reaction of  $HOCl$  with ABTS compared to those of  $Mn(VII)$  and  $Fe(VI)$ .<sup>25,30</sup>

Overall, the results obtained in this study suggest that ABTS not only serves as a novel and efficient electron shuttle to catalyze the permanganation process for the treatment of phenolic compounds containing waters over a wide pH range but also acts as a one-electron-transfer probe to provide useful information for the fates of the manganese intermediates in  $Mn(VII)$  oxidation. The promoting effect of ABTS on the oxidation kinetics of phenol by  $Mn(VII)$  was also confirmed in natural water (Figure S11), suggesting that  $ABTS^{\bullet+}$  was not readily quenched by water matrix components. Recent studies have successfully developed the ABTS-modified carbon nanotubes (CNTs) for catalytic technology,<sup>53–57</sup> suggesting that heterogeneous ABTS catalysts (e.g., ABTS-loaded carbons) may be an option for water treatment. This issue needs further investigations by considering redox potential change and mass transfer related to heterogeneous ABTS catalysts. However, the high cost and unknown toxicity of the synthetic mediator, ABTS, may hinder its utilization. Nevertheless, this work brings about the convenience to find out the low-cost and environmentally friendly natural mediators for further development of  $Mn(VII)$ -mediator system, as was done in the case of laccase by Gutiérrez et al.<sup>58</sup> Humic substances exist ubiquitously in soils and waters,<sup>59</sup> and they can act as redox mediators participating in various chemical and biochemical processes.<sup>60,61</sup> Previous studies have showed that isolated humic acid (HA) could also greatly accelerate the oxidation of phenols by  $Mn(VII)$  under slightly acidic conditions, which was mainly ascribed to its roles as both a reductant and a complexing agent.<sup>4,5,9</sup> On the basis of the results obtained with ABTS, a model mediator,<sup>62,63</sup> it seems likely that HA may also promote  $Mn(VII)$  oxidation of phenols under slightly acidic condition through a catalytic mechanism via the pair (HA and  $HA_{ox}$ ) analogous to the pairing of ABTS and  $ABTS^{\bullet+}$  (Figure S12), which needs further studies. In addition,

because of the high reactivity of ABTS<sup>•+</sup> with phenolic moieties, it is recommended that the ABTS colorimetric method to quantify water oxidants in trace levels in natural waters or in well-defined laboratory solutions should be conducted under the conditions of acidic pH as well as with ABTS in excess (i.e., a high ratio of ABTS<sub>0</sub> to ABTS<sup>•+</sup>) to avoid the appreciable decay of ABTS<sup>•+</sup>.

## ■ ASSOCIATED CONTENT

### 📄 Supporting Information

The Supporting Information is available free of charge on the ACS Publications website at DOI: 10.1021/acs.est.5b03358.

Additional information on the kinetic analysis for the formation of ABTS<sup>•+</sup> in the reaction of Mn(VII) with ABTS, reaction kinetics between ABTS<sup>•+</sup> and phenol, linear free-energy relationships, and the effect of different phenol concentrations on phenol oxidation by Mn(VII) and ABTS. Tables showing the constants for reactions of Mn(VII), ABTS, and ABTS<sup>•+</sup> and stoichiometries of the reaction of ABTS<sup>•+</sup> with phenol. Figures showing the decay of ABTS<sup>•+</sup>, a linear plot of the pseudo-first-order rate constant for the decay of ABTS<sup>•+</sup>, the second-order rate constant for the reactions of ABTS<sup>•+</sup> with selected phenolic compounds, correlations between the second-order rate constants for ABTS<sup>•+</sup> with undissociated phenols, oxidation kinetics, and the effects of ABTS or humic acid on Mn(VII) oxidation. (PDF)

## ■ AUTHOR INFORMATION

### Corresponding Authors

\*Tel: 86-451-86283010; fax: 86-451-86283010; email: jiangjin@hit.edu.cn.

\*E-mail: majun@hit.edu.cn.

### Notes

The authors declare no competing financial interest.

## ■ ACKNOWLEDGMENTS

This work was financially supported by the National Science & Technology Pillar Program of China (no. 2012BAC05B02), the National Natural Science Foundation of China (51578203 and 51208159), Heilongjiang Province Natural Science Foundation (QC2014C055), the Postdoctoral Science Foundation and the Special Financial Grant of China (2013MS41402 and 2015T80366), Heilongjiang Province Postdoctoral Science Foundation (LBH-Z13115), the Funds of State Key Laboratory of Urban Water Resource and Environment (HIT, 2013TS04), the Foundation for the Author of National Excellent Doctoral Dissertation of China (201346), and the Fundamental Research Funds for the Central Universities.

## ■ REFERENCES

- (1) Hu, L.; Martin, H. M.; Arce-Bulted, O.; Sugihara, M. N.; Keating, K. A.; Strathmann, T. J. Oxidation of carbamazepine by Mn(VII) and Fe(VI): Reaction kinetics and mechanism. *Environ. Sci. Technol.* **2009**, *43* (2), 509–515.
- (2) Hu, L.; Martin, H. M.; Strathmann, T. J. Oxidation kinetics of antibiotics during water treatment with potassium permanganate. *Environ. Sci. Technol.* **2010**, *44* (16), 6416–6422.
- (3) Rodríguez, E.; Majado, M. E.; Meriluoto, J.; Acero, J. L. Oxidation of microcystins by permanganate: Reaction kinetics and implications for water treatment. *Water Res.* **2007**, *41* (1), 102–110.

- (4) Jiang, J.; Pang, S.; Ma, J. Oxidation of triclosan by permanganate (Mn(VII)): Importance of ligands and in situ formed manganese oxides. *Environ. Sci. Technol.* **2009**, *43* (21), 8326–8331.

- (5) Jiang, J.; Pang, S.; Ma, J. Role of ligands in permanganate oxidation of organics. *Environ. Sci. Technol.* **2010**, *44* (11), 4270–4275.

- (6) Jiang, J.; Pang, S.; Ma, J.; Liu, H. Oxidation of phenolic endocrine disrupting chemicals by potassium permanganate in synthetic and real waters. *Environ. Sci. Technol.* **2012**, *46* (3), 1774–1781.

- (7) Pang, S.; Jiang, J.; Gao, Y.; Zhou, Y.; Huangfu, X.; Liu, Y.; Ma, J. Oxidation of flame retardant tetrabromobisphenol A by aqueous permanganate: Reaction kinetics, brominated products, and pathways. *Environ. Sci. Technol.* **2014**, *48* (1), 615–623.

- (8) Jiang, J.; Gao, Y.; Pang, S.; Wang, Q.; Huangfu, X.; Liu, Y.; Ma, J. Oxidation of bromophenols and formation of brominated polymeric products of concern during water treatment with potassium permanganate. *Environ. Sci. Technol.* **2014**, *48* (18), 10850–10858.

- (9) Pang, S. Y.; Wang, Q.; Jiang, J. The confounding effects of dissolved humic acid on the oxidation of simple substituted phenols by permanganate: Comment on “Reinvestigation of the role of humic acid in the oxidation of phenols by permanganate. *Environ. Sci. Technol.* **2014**, *48* (11), 6518–6519.

- (10) Jiang, J.; Gao, Y.; Pang, S.; Lu, X.; Zhou, Y.; Ma, J.; Wang, Q. Understanding the role of manganese dioxide in the oxidation of phenolic compounds by aqueous permanganate. *Environ. Sci. Technol.* **2015**, *49* (1), 520–528.

- (11) Waldemer, R. H.; Tratnyek, P. G. Kinetics of contaminant degradation by permanganate. *Environ. Sci. Technol.* **2006**, *40* (3), 1055–1061.

- (12) Zhang, J.; Sun, B.; Guan, X.; Wang, H.; Bao, H.; Huang, Y.; Qiao, J.; Zhou, G. Ruthenium nanoparticles supported on CeO<sub>2</sub> for catalytic permanganate oxidation of butylparaben. *Environ. Sci. Technol.* **2013**, *47* (22), 13011–13019.

- (13) Kersten, P. J.; Kalyanaraman, B.; Hammel, K. E.; Reinhammar, B.; Kirk, T. K. Comparison of lignin peroxidase, horseradish peroxidase and laccase in the oxidation of methoxybenzenes. *Biochem. J.* **1990**, *268* (2), 475–480.

- (14) Bourbonnais, R.; Paice, M. G.; Freiermuth, B.; Bodie, E.; Borneman, S. Reactivities of various mediators and laccases with kraft pulp and lignin model compounds. *Appl. Environ. Microb.* **1997**, *63* (12), 4627–4632.

- (15) Bourbonnais, R.; Paice, M. G. Oxidation of non-phenolic substrates: An expanded role for laccase in lignin biodegradation. *FEBS Lett.* **1990**, *267* (1), 99–102.

- (16) Riva, S. Laccases: Blue enzymes for green chemistry. *Trends Biotechnol.* **2006**, *24* (5), 219–226.

- (17) Pickard, M. A.; Roman, R.; Tinoco, R.; Vazquez-Duhalt, R. Polycyclic aromatic hydrocarbon metabolism by white rot fungi and oxidation by *Coriolopsis gallica* UAMH 8260 laccase. *Appl. Environ. Microb.* **1999**, *65* (9), 3805–3809.

- (18) Collins, P. J.; Kotterman, M.; Field, J. A.; Dobson, A. Oxidation of anthracene and benzo[a]pyrene by laccases from *Trametes versicolor*. *Appl. Environ. Microb.* **1996**, *62* (12), 4563–4567.

- (19) Majcherczyk, A.; Johannes, C.; Hüttermann, A. Oxidation of polycyclic aromatic hydrocarbons (PAH) by laccase of *Trametes versicolor*. *Enzyme Microb. Technol.* **1998**, *22* (5), 335–341.

- (20) Jeon, J.; Murugesan, K.; Kim, Y.; Kim, E.; Chang, Y. Synergistic effect of laccase mediators on pentachlorophenol removal by *Ganoderma lucidum* laccase. *Appl. Microbiol. Biotechnol.* **2008**, *81* (4), 783–790.

- (21) Keum, Y. S.; Li, Q. X. Fungal laccase-catalyzed degradation of hydroxy polychlorinated biphenyls. *Chemosphere* **2004**, *56* (1), 23–30.

- (22) Camarero, S.; Ibarra, D.; Martínez, M. J.; Martínez, Á. T. Lignin-derived compounds as efficient laccase mediators for decolorization of different types of recalcitrant dyes. *Appl. Environ. Microb.* **2005**, *71* (4), 1775–1784.

- (23) Murugesan, K.; Arulmani, M.; Nam, I.; Kim, Y.; Chang, Y.; Kalaichelvan, P. T. Purification and characterization of laccase produced by a white rot fungus *Pleurotus sajor-caju* under submerged culture

condition and its potential in decolorization of azo dyes. *Appl. Microbiol. Biotechnol.* **2006**, *72* (5), 939–946.

(24) Murugesan, K.; Nam, I.; Kim, Y.; Chang, Y. Decolorization of reactive dyes by a thermostable laccase produced by *Ganoderma lucidum* in solid state culture. *Enzyme Microb. Technol.* **2007**, *40* (7), 1662–1672.

(25) Lee, Y.; Kissner, R.; von Gunten, U. Reaction of ferrate(VI) with ABTS and self-decay of ferrate(VI): Kinetics and mechanisms. *Environ. Sci. Technol.* **2014**, *48* (9), 5154–5162.

(26) Thompson, G. W.; Ockerman, L. T.; Schreyer, J. M. Preparation and purification of potassium ferrate. VI. *J. Am. Chem. Soc.* **1951**, *73* (3), 1379–1381.

(27) Sharma, V. K. Oxidation of inorganic contaminants by ferrates (VI, V, and IV)-kinetics and mechanisms: A review. *J. Environ. Manage.* **2011**, *92* (4), 1051–1073.

(28) Lee, Y.; Zimmermann, S. G.; Kieu, A. T.; von Gunten, U. Ferrate (Fe(VI)) application for municipal wastewater treatment: A novel process for simultaneous micropollutant oxidation and phosphate removal. *Environ. Sci. Technol.* **2009**, *43* (10), 3831–3838.

(29) Gallard, H.; von Gunten, U. Chlorination of phenols: Kinetics and formation of chloroform. *Environ. Sci. Technol.* **2002**, *36* (5), 884–890.

(30) Pinkernell, U.; Nowack, B.; Gallard, H.; von Gunten, U. Methods for the photometric determination of reactive bromine and chlorine species with ABTS. *Water Res.* **2000**, *34* (18), 4343–4350.

(31) Lee, Y.; Yoon, J.; von Gunten, U. Spectrophotometric determination of ferrate (Fe(VI)) in water by ABTS. *Water Res.* **2005**, *39* (10), 1946–1953.

(32) Re, R.; Pellegrini, N.; Proteggente, A.; Pannala, A.; Yang, M.; Rice-Evans, C. Antioxidant activity applying an improved ABTS radical cation decolorization assay. *Free Radical Biol. Med.* **1999**, *26* (9–10), 1231–1237.

(33) Klewicki, J. K.; Morgan, J. J. Kinetic behavior of Mn(III) complexes of pyrophosphate, EDTA, and citrate. *Environ. Sci. Technol.* **1998**, *32* (19), 2916–2922.

(34) Lee, D. G.; Brownridge, J. R. Oxidation of hydrocarbons. IV. Kinetics and mechanism of the oxidative cleavage of cinnamic acid by acidic permanganate. *J. Am. Chem. Soc.* **1974**, *96* (17), 5517–5523.

(35) Lee, D. G.; Chen, T. Reduction of manganate(VI) by mandelic acid and its significance for development of a general mechanism of oxidation of organic compounds by high-valent transition metal oxides. *J. Am. Chem. Soc.* **1993**, *115* (24), 11231–11236.

(36) Lee, D. G.; Sebastián, C. F. The oxidation of phenol and chlorophenols by alkaline permanganate. *Can. J. Chem.* **1981**, *59* (18), 2776–2779.

(37) Lee, D. G.; Chen, T. Oxidation of hydrocarbons. 18. Mechanism of the reaction between permanganate and carbon-carbon double bonds. *J. Am. Chem. Soc.* **1989**, *111* (19), 7534–7538.

(38) von Gunten, U. Ozonation of drinking water: Part I. Oxidation kinetics and product formation. *Water Res.* **2003**, *37* (7), 1443–1467.

(39) Reisz, E.; Leitzke, A.; Jarocki, A.; Irmscher, R.; von Sonntag, C. Permanganate formation in the reactions of ozone with Mn(II): A mechanistic study. *Aqua* **2008**, *57* (6), 451–464.

(40) Davies, G. Some aspects of the chemistry of manganese(III) in aqueous solution. *Coord. Chem. Rev.* **1969**, *4* (2), 199–224.

(41) Tian, X.; Schaich, K. M. Effects of molecular structure on kinetics and dynamics of the trolox equivalent antioxidant capacity assay with ABTS<sup>•+</sup>. *J. Agric. Food Chem.* **2013**, *61* (23), 5511–5519.

(42) Scott, S. L.; Chen, W. J.; Bakac, A.; Espenson, J. H. Spectroscopic parameters, electrode potentials, acid ionization constants, and electron exchange rates of the 2,2'-azinobis(3-ethylbenzothiazoline-6-sulfonate) radicals and ions. *J. Phys. Chem.* **1993**, *97* (25), 6710–6714.

(43) Dean, J. A. *Lange's Handbook of Chemistry*. McGraw-Hill: New York, 1985.

(44) Stone, A. T. Reductive dissolution of manganese(III/IV) oxides by substituted phenols. *Environ. Sci. Technol.* **1987**, *21* (10), 979–988.

(45) Gallard, H.; Pellizzari, F.; Croué, J. P.; Legube, B. Rate constants of reactions of bromine with phenols in aqueous solution. *Water Res.* **2003**, *37* (12), 2883–2892.

(46) Tratnyek, P. G.; Hoigné, J. Kinetics of reactions of chlorine dioxide (OCIO) in water—II. Quantitative structure-activity relationships for phenolic compounds. *Water Res.* **1994**, *28* (1), 57–66.

(47) Lee, Y.; von Gunten, U. Oxidative transformation of micropollutants during municipal wastewater treatment: Comparison of kinetic aspects of selective (chlorine, chlorine dioxide, ferrate<sup>VI</sup>, and ozone) and non-selective oxidants (hydroxyl radical). *Water Res.* **2010**, *44* (2), 555–566.

(48) Hansch, C.; Leo, A.; Taft, R. W. A survey of Hammett substituent constants and resonance and field parameters. *Chem. Rev.* **1991**, *91* (2), 165–195.

(49) Lee, Y.; Yoon, J.; von Gunten, U. Kinetics of the oxidation of phenols and phenolic endocrine disruptors during water treatment with ferrate (Fe(VI)). *Environ. Sci. Technol.* **2005**, *39* (22), 8978–8984.

(50) Hoigné, J.; Bader, H. Rate constants of reactions of ozone with organic and inorganic compounds in water—II: Dissociating organic compounds. *Water Res.* **1983**, *17* (2), 185–194.

(51) Hoigné, J.; Bader, H. Kinetics of reactions of chlorine dioxide (OCIO) in water—I. Rate constants for inorganic and organic compounds. *Water Res.* **1994**, *28* (1), 45–55.

(52) Du, J.; Sun, B.; Zhang, J.; Guan, X. Parabola-like shaped pH-rate profile for phenols oxidation by aqueous permanganate. *Environ. Sci. Technol.* **2012**, *46* (16), 8860–8867.

(53) Karnicka, K.; Miecznikowski, K.; Kowalewska, B.; Skunik, M.; Opallo, M.; Rogalski, J.; Schuhmann, W.; Kulesza, P. J. ABTS-modified multiwalled carbon nanotubes as an effective mediating system for bioelectrocatalytic reduction of oxygen. *Anal. Chem.* **2008**, *80* (19), 7643–7648.

(54) Nazaruk, E.; Sadowska, K.; Madrak, K.; Biernat, J. F.; Rogalski, J.; Bilewicz, R. Composite bioelectrodes based on lipidic cubic phase with carbon nanotube network. *Electroanalysis* **2009**, *21* (3–5), 507–511.

(55) Deng, W.; Tan, Y.; Fang, Z.; Xie, Q.; Li, Y.; Liang, X.; Yao, S. ABTS-multiwalled carbon nanotubes nanocomposite/Bi film electrode for sensitive determination of Cd and Pb by differential pulse stripping voltammetry. *Electroanalysis* **2009**, *21* (22), 2477–2485.

(56) Sadowska, K.; Stolarczyk, K.; Biernat, J. F.; Roberts, K. P.; Rogalski, J.; Bilewicz, R. Derivatization of single-walled carbon nanotubes with redox mediator for biocatalytic oxygen electrodes. *Bioelectrochemistry* **2010**, *80* (1), 73–80.

(57) Nazaruk, E.; Sadowska, K.; Biernat, J. F.; Rogalski, J.; Ginalska, G.; Bilewicz, R. Enzymatic electrodes nanostructured with functionalized carbon nanotubes for biofuel cell applications. *Anal. Bioanal. Chem.* **2010**, *398* (4), 1651–1660.

(58) Gutiérrez, A.; Del Río, J. C.; Ibarra, D.; Rencoret, J.; Romero, J.; Speranza, M.; Camarero, S.; Martínez, M. J.; Martínez, Á. T. Enzymatic removal of free and conjugated sterols forming pitch deposits in environmentally sound bleaching of eucalypt paper pulp. *Environ. Sci. Technol.* **2006**, *40* (10), 3416–3422.

(59) Matilainen, A.; Gjessing, E. T.; Lahtinen, T.; Hed, L.; Bhatnagar, A.; Sillanpää, M. An overview of the methods used in the characterisation of natural organic matter (NOM) in relation to drinking water treatment. *Chemosphere* **2011**, *83* (11), 1431–1442.

(60) Aeschbacher, M.; Sander, M.; Schwarzenbach, R. P. Novel electrochemical approach to assess the redox properties of humic substances. *Environ. Sci. Technol.* **2010**, *44* (1), 87–93.

(61) Aeschbacher, M.; Graf, C.; Schwarzenbach, R. P.; Sander, M. Antioxidant properties of humic substances. *Environ. Sci. Technol.* **2012**, *46* (9), 4916–4925.

(62) Cañas, A. I.; Alcalde, M.; Plou, F.; Martínez, M. J.; Martínez, Á. T.; Camarero, S. Transformation of polycyclic aromatic hydrocarbons by laccase is strongly enhanced by phenolic compounds present in soil. *Environ. Sci. Technol.* **2007**, *41* (8), 2964–2971.

(63) Camarero, S.; Cañas, A. I.; Nousiainen, P.; Record, E.; Lomascolo, A.; Martínez, M. J.; Martínez, Á. T. p-Hydroxycinnamic acids as natural mediators for laccase oxidation of recalcitrant compounds. *Environ. Sci. Technol.* **2008**, *42* (17), 6703–6709.